NJC

Accepted Manuscript

This article can be cited before page numbers have been issued, to do this please use: M. E. Villanueva, G. J. Copello and V. Campo Dall´Orto, *New J. Chem.*, 2018, DOI: 10.1039/C8NJ02332H.

This is an Accepted Manuscript, which has been through the Royal Society of Chemistry peer review process and has been accepted for publication.

Accepted Manuscripts are published online shortly after acceptance, before technical editing, formatting and proof reading. Using this free service, authors can make their results available to the community, in citable form, before we publish the edited article. We will replace this Accepted Manuscript with the edited and formatted Advance Article as soon as it is available.

You can find more information about Accepted Manuscripts in the author guidelines.

Please note that technical editing may introduce minor changes to the text and/or graphics, which may alter content. The journal's standard Terms & Conditions and the ethical guidelines, outlined in our author and reviewer resource centre, still apply. In no event shall the Royal Society of Chemistry be held responsible for any errors or omissions in this Accepted Manuscript or any consequences arising from the use of any information it contains.

ROYAL SOCIETY OF CHEMISTRY

rsc.li/njc

View Article Online
DOI: 10.1039/C8NJ02332H

Journal Name

ARTICLE

Solar light efficient photocatalytic activity degradation of emergent contaminants by coated TiO_2 nanoparticles†

Received 00th January 20xx,
Accepted 00th January 20xx

DOI: 10.1039/x0xx00000x
www.rsc.org/

María Emilia Villanueva,[a,b] Guillermo Javier Copello [a,b] and Viviana Campo Dall´Orto [a,b,*]

The photocatalytic degradation of different emergent contaminants in aqueous solutions has been studied by using *oligomer*-coated TiO_2 nanoparticles under solar light irradiation. The *oligomer* was synthesized using methacrylic acid, ethylene glycol diglycidyl ether and imidazole. The material was characterized by SEM, DLS, FT-IR and FT-Raman and UV-Vis spectroscopy. The photocatalytic behavior on the model azo-dye Methyl Orange was analyzed in different conditions (initial concentration and pH) and the kinetic parameters were described by using the Langmuir-Hinshelwood model. The reuse and photocorrosion of the nanoparticles was studied up to seven operative cycles. The *oligomer*-coated nanoparticles showed better performance than the uncoated ones due to an increment in absorption in the visible light region. The charge transfer process would form electron / hole pairs (e- / h^+) with the holes localized on the organic ligands (most probably on imidazole residues from *oligomers*) and the electrons in the conduction band of TiO_2. Supernatant safety after the photocatalytic treatment was examined by the lettuce seeds assay and no toxicity was found. The versatility of the material was studied by exposing it to different emergent contaminants (Ciprofloxacin, Trimethoprim and Chloramphenicol).

Keywords: photocatalysis; TiO_2 nanoparticles; solar light irradiation; oligomers; LMCT complexes.

Introduction

The raising use pharmaceuticals, personal care products and endocrine disrupting compounds brings with it several environmental issues, since they can persist in the environment after their disposal [1]. These chemicals that had not been previously detected in water supplies (or were found in far lower concentrations) and nowadays are discovered either in surface water or groundwater, are known as emerging contaminants [2,3]. Among the pharmaceutical products, many antibiotics, such as ciprofloxacin, trimethoprim and chloramphenicol, had been classified as emerging contaminants [4].

Advanced oxidation technologies (AOT), including heterogeneous photocatalytic degradation, have become attractive remediation technologies for wastewater treatment. Since TiO_2 nanoparticles (TiO_2 NP) are relatively inexpensive and highly effective, they are one of the most commonly found photocatalysts in the literature [5]. They have received much attention in the degradation and mineralization of environmental contaminants [6–8]. Their catalytic activity is expected to be improved not only because of their high surface area, but also because of changes in surface properties, such as surface defects, crystallinity, morphology, pore distribution, band gap energy and type and proportion of -OH groups at the surface [9,10].

It has been well demonstrated that when TiO_2 is irradiated, electrons are promoted from the valence band to the conduction band to give electron-hole pairs. The holes (h^+) at the TiO_2 valence band, can oxidize water or hydroxide to produce hydroxyl radicals ($OH^\bullet$). The hydroxyl radical is a powerful oxidizing agent that attacks organic compounds to form intermediates and/or final products. The intermediates can also react with $OH^\bullet$ to produce final products [11].

One of the limiting points in the expansion and application of heterogeneous photocatalysis developments is that the nanoparticles of TiO_2 (TiO_2 NP) undergo more efficient activation when irradiated by UV (λ<388 nm) than visible light, due to the wide band gap energy. This imply that less than 5 % of the incident solar light can be used in the oxidation process.[12] Aiming to overcome this drawback, various modification methods have been studied to enhance the photocatalytic activity and performance of TiO_2 under solar-light irradiation.

The electronic band gap of TiO_2 can be modified by *N*-doping,

[a] Universidad de Buenos Aires, Facultad de Farmacia y Bioquímica, Departamento de Química Analítica y Fisicoquímica, Buenos Aires, Argentina;
[b] CONICET – Universidad de Buenos Aires, Instituto de Química y Metabolismo del Fármaco, (IQUIMEFA); Buenos Aires, Argentina.

† Electronic Supplementary Information (ESI) available: [details of any supplementary information available should be included here]. See DOI: 10.1039/x0xx00000x

View Article Online
DOI: 10.1039/C8NJ02332H

creating intermediate levels between valence band and conduction band [13]. The electrons injected into the TiO_2 conduction band can also reduce the O_2 to the superoxide anion ($O_2^{\bullet -}$). The holes formed from transition (h^+) react with OH^- to produce $OH^\bullet$, the reactive species responsible for dyes degradation under visible light irradiation.[13]

In a completely different approach, in order to achieve visible light sensitization, dyes or small sensitizing molecules are adsorbed on previously prepared TiO_2 crystalline NPs.[14] Small organic molecules (carboxylic acids, phenols) adsorbed on the oxide surface form a charge transfer complex that absorbs in the visible region at a lower energy than either the chelating molecules or the oxide particles. In this case, direct injection of an electron from the ground state of the molecule into the conduction band of the oxide occurs without involvement of any excited molecular state.[15–18]

The *N*-heterocycle is particularly reactive and can be converted to radical cation stabilized by resonance. Dogan *et al* oxidized 1-methylimidazole to a radical cation which could react with $OH^\bullet$ or with OH^- at high pH values.[19]

The aim of this work was to develop a TiO_2 NP coating which enhanced the absorbance in the visible light region, in order to use sunlight as a more efficient light source. It was based on a synthesized *oligomer* composed by methacrylic acid (MAA), the diepoxide ethylenglycol diglycidyl ether (EGDE) and imidazole (IM), named (EGDE-IM-*co*-MAA) *oligomers*. The coated TiO_2 NPs described were deeply characterized, and the photocatalytic performance on an azo-dye decomposition was evaluated and compared with uncoated NPs. The versatility of the photocatalytic behavior was studied using the emerging contaminants chloramphenicol, ciprofloxacin and trimethoprim.

Experimental

Materials. Ethylene glycol diglycidyl ether (EGDE; 50 wt% in ethylene glycol dimethyl ether; MW: 174.197; 12.1% oxirane oxygen; SW: 1.1891) was purchased from TCI America. Imidazole (IM; 99 wt%; MW: 68.077) and methacrylic acid (MAA; 99 wt%; MW: 86.09; SW: 1.015) were purchased from Sigma–Aldrich. Benzoyl peroxide was obtained from Fluka. Acetonitrile from Baxter was of HPLC grade. TiO_2 NP (AEROXIDE TiO_2 P25, Evonik) were kindly donated by Evonik Degussa Argentina SA. 5,5-dimethyl-1-pyrroline-N oxide (DMPO) was purchased from Sigma-Aldrich. Methyl Orange (MO) was from Santa Cruz Biotechnology, Inc. Ciprofloxacin, trimethoprim and chloramphenicol were acquired in Saporiti (Argentina).

Synthesis of (EGDE-IM-*co*-MAA) *oligomers* and TiO_2 NP coating. The (EGDE-IM-*co*-MAA) *oligomers* were synthesized in agreement with previously published work.[20] In order to prepare the coated NP, 250 mg of TiO_2 NP where exposed to a 0.1 N NaOH solution for 30 min. After that time, the NP were washed three times with deionized water. Then, the NP were left in contact with a 25 mg mL^{-1} *oligomer* aqueous solution for 18 h. Afterwards, the NP were rinsed three times with water and dried at 37 ºC.

FTIR and Raman spectroscopy. Attenuated total reflectance Fourier Transform Infra Red (ATR-FTIR) spectra (diamond attenuated total reflectance) of uncoated and coated NP, before and after the photocatalysis assay, were recorded using a Nicolet iS50 Advanced Spectrometer (Thermo Scientific). ATR-FTIR spectra were recorded with 32 scans and a resolution of 1 cm^{-1}. FT-Raman spectra of uncoated and coated NP, before and after the photocatalysis assay, were acquired with an excitation laser beam of 1064 nm, 0.5 W laser power, resolution of 4 cm^{-1}, 500 scans. All samples were previously dried for 24 h at 60 ºC to avoid the interference of water related bands.

Microscopical characterization. Scanning Electron Microscopy (SEM) images of dried and gold coated samples were taken using a Quanta FEG 250 microscope.

Dynamic Light Scattering. The uncoated and coated NP were analyzed by Dynamic Light Scattering (DLS, Zetasizer Nano-Zs, Malvern Instruments, Worcestershire, UK).

Electron spin resonance (ESR). The coated and uncoated NP were placed in a vial with distilled water, left in agitation for 30 min in the darkness and then exposed to solar-light for 30 min. At this moment, an aliquot of 32 µL of supernatant was mixed with 16 µL of 3 M DMPO (spin trap), and the continuous wave (CW) ESR spectra of the DMPO spin adducts were recorded at 20 °C, 8 min after the end of incubation, in the X-band ESR spectrometer Bruker EMX plus (Bruker Instruments, Inc., Berlin, Germany).

The spectrometer settings were: center field: 3515 G, sweep width: 100 G, microwave power: 10 mW, microwave frequency: 9.85 GHz, conversion time: 2.56 ms, time constant: 2.56 ms, modulation frequency: 50 kHz, modulation amplitude: 0.11 G, gain: 2.00×10^4, resolution: 1024 points. All spectra were the accumulation of 20 scans.

Optical absorption spectra. UV-Vis absorption spectra of uncoated and coated TiO_2 nanoparticles suspensions were collected on an Evolution Array UV–visible Spectrophotometer Thermo Scientific spectrophotometer from 200 to 600 nm.[21]

Point of zero charge (PZC). Each initial solution consisted in ten milliliters of 0.01 M NaCl that had been boiled to remove dissolved CO_2 and then cooled to room temperature. The pH was adjusted to a value between 4 and 8 using 0.1 M HCl or 0.1 M NaOH and their pH was recorded (initial pH). Then, 10 mg of coated and uncoated NPs were immersed in each solution and the drift in the pH after 48 h was measured. Since the addition of a solid into a solution (with a particular pH) induces a shift in the pH in the direction of the PZC, then the pH at which the addition of the sample did not induce a shift in the pH was taken as the PZC.

Photocatalytic Experiments. The photocatalytic activities were evaluated by the decomposition of the azo dye Methyl Orange (MO) as a model drug under solar light in Buenos Aires city from January to April. Aqueous solutions of MO (50 mL, 0.0121-0.0595 mg L^{-1}) were placed in a vessel, and 10 ± 2 mg of uncoated or coated NP was added. Prior to irradiation, the suspensions were magnetically stirred in the dark for about 30 min. The suspensions were kept under constant air-equilibrated conditions before and during illumination. At certain time intervals, aliquots were sampled and centrifuged to remove particles. The supernatants were analyzed by recording the UV-vis spectra and monitoring variations in the maximum band (463 nm). This assay was conducted in different conditions in order to evaluate the NP performance. Different concentrations of MO, interaction times and values of pH (4.0, 5.5, 7.0 and 8.5) were evaluated and the reused material was also tested in order to evaluate photocorrosion (interaction time 1 h). A control with a vessel containing only the *oligomer* solution was also performed.

The versatility of the photocatalytic activity was studied by exposing the samples to 0.2 M solutions of chloramphenicol, trimethoprim and ciprofloxacin. The photodegradation of the drugs was studied

View Article Online
DOI: 10.1039/C8NJ02332H
Journal Name ARTICLE

by exposing the antibiotics solutions to sunlight during 1 h. The same experiment was conducted in dark conditions as a control.

MO adsorption in dark conditions. In order to evaluate if the material adsorbed the dye in its surface, 10 ± 2 mg of uncoated or coated NP were left in contact with a 0.0272 mg L^{-1} MO solution for 48 h in the dark. After that time, the supernatant was centrifuged to remove the particles and analyzed by recording variations in the maximum absorption band (463 nm) using a UV–Vis Spectrophotometer.

Short-term toxicity screening of hazardous-waste sites. This assay was performed in order to analyze the toxicity of the treated solutions after the photocatalytic process. Residual water after MO photocatalytic degradation with coated and uncoated NP was evaluated. Distilled water was used as a control. The test was performed as follows: a piece of filter paper was placed in a petri dish and 40 lettuce seeds were evenly distributed over the paper and were covered with another piece of filter paper. The tested solutions were poured in the Petri dishes, covered and stored in a dark and undisturbed environment for one week to let the seeds germinate. After that time, the number of germinated seeds in each Petri dish was counted [22].

Photoluminescence. The fluorescence spectrophotometer (Perkin Elmer) was used to record the PL spectra with an excitation wavelength of 320 nm.

Total Organic Content (TOC). The Total Organic Content was analyzed using an Analytical technologies TOC-1030C analyzer.

Statistics. All quantitative results were obtained from triplicate samples. Data were expressed as means ± SD. Statistical analysis was carried out using a One-way ANOVA test and a Bonferroni post test. A value of $p < 0.05$ was considered to be statistically significant.

Results and discussion

FTIR and FT-Raman spectroscopy. In the uncoated NP FT-IR spectrum (Figure S1) the characteristic TiO_2 NP bands could be found. It could be seen peaks corresponding to stretching vibrations of the O-H and bending vibrations of the adsorbed water molecules at 3422 cm^{-1} and 1645 cm^{-1}, respectively. The broad band at 1351 cm^{-1} was due to Ti-O-Ti vibrations [23,24]. On the other the hand, in the coated NP sample, a different spectrum could be observed (Figure S1 and S2). Although the band corresponding to the O-H stretching vibrations was also present, other bands corresponding to the *oligomer* coating could be found, such as the bands at 2932 and 2878 cm^{-1} from the vibration of CH_3 and CH_2, at 1715 cm^{-1} from C=O symmetric stretching of carboxylic groups, at 1573 cm^{-1} from C=C and/or C=N stretching and to the asymmetric stretching of carboxylate from MAA, at 1287 cm^{-1} from CH, at 1234 cm^{-1} from CN and CH, and at 1100 cm^{-1} from C-O-C [25–27]. These results showed that the coating process was successful.

The splitting between the asymmetric and symmetric stretching of C=O bands of the carboxylate groups present in the coated NP spectrum can indicate the existence of bidentate interaction in complexes, if the gap between peaks lies between 50-150 cm^{-1} [18]. The TiO_2-acetylacetonate hybrid material reported by Sannino *et al* was a polymeric network of titanium oxoclusters, on the surface of which part of the Ti^{4+} ions were involved in a strong complexation with acetylacetonate ligands, with a peak gap of 147 cm^{-1}. Here in the case of coated NP, the mentioned gap was of 142 cm^{-1}, evidencing an interaction between Ti(IV) from TiO_2 NP and the (EGDE-IM-*co*-MAA) *oligomers*.

The FT- Raman spectra can be observed in Figure S3. The bands at 157, 202, 406, 520, and 647 cm^{-1} were observed. These bands were assigned to the anatase phase, and they can be attributed to the five Raman-active modes of anatase phase with the symmetries of E_g, E_g, B_{1g}, A_{1g}, and E_g, respectively [28]. The presence of a broad band between 3050 and 2800 cm^{-1} in the coated NP spectrum corresponded to C-H motives, which confirmed the presence of (EGDE-IM-*co*-MAA) *oligomers* in the coating.

Microscopical characterization. Figure S4 shows the SEM images of uncoated and coated NP. The average size of uncoated NP was 83.7 ± 15.9 nm and in the case of coated NP it was 89.5 ± 16.6 nm. As it can be seen, the difference in size and aspect between them was negligible. However, the inspection of the whole samples showed that the coated NP were more agglomerated than uncoated ones. This could be directly related with the functionalities of the (EGDE-IM-*co*-MAA) *oligomers*. These hydrophilic molecules bear carboxylic groups from MAA, together with positive residues such as protonated imidazole units (IMH^+). These oppositely charged residues attached to a flexible network forming a layer on NP surface could be oriented in the best way to minimize the surface energy, enhancing the electrostatic interaction between particles. Besides, -OH groups resulting from epoxide opening on EGDE molecules could form H-bonds that reinforce the association and particles aggregation.

Dynamic Light Scattering and Zeta potential analysis. The zeta potential values obtained in this experiment provided evidence for the efficacy of the NP coating. The zeta potential value at pH 7.0 of uncoated NP was -15.00 ± 0.86 mV and in the case of coated NP it was -7.97 ± 0.31 mV. The shift of zeta potential at pH 7.0 as a result of coating can be explained by considering the nature of the (EGDE-IM-*co*-MAA) *oligomers*. The bulk *oligomer* solution is a heterogeneous mixture of molecules: some with prevalence of MAA chains, others with prevalence of (EGDE-IM) adducts. In the last case, two types of IM residues can be present: *N*-monosubstituted imidazole units either neutral (IM) or protonated (IMH^+); and *N,N*-disubstituted imidazole units, bearing permanent positive charge (IM^+).[20] Thus, when *oligomers* from bulk solution interacted with the negatively charged NP, those molecules with prevalence of IM^+ and /or IMH^+ residues were electrostatically attracted by the negative surface and were expected to neutralize in some extent the surface charge. This could be the reason for the less negative zeta potential of coated NP.[29] The *oligomers* adsorbed on NP would present most of their IM^+/IMH^+ groups oriented towards the negative surface of NP, and any $-CO_2^-$ group from MAA oriented towards the solution.

The hydrodynamic diameter obtained by DLS was 186.6 ± 8.0 nm for uncoated NP and 1133.0 ± 78.8 nm for coated NP. These results were in contrast with those observed in the SEM images where the coated NP and uncoated NP showed a similar size. The difference between these two assays could have been due to the low

View Article Online
DOI: 10.1039/C8NJ02332H

dispersibility of TiO_2 and the agglomeration experienced by the coated NP proving that the *oligomer* coating was present.

Solar-light effect on photocatalytic experiments. Adsorption experiments in dark condition were carried out for MO. For this dye, the loading on the uncoated and coated NP was negligible, indicating that the adsorption process could not be detected by this

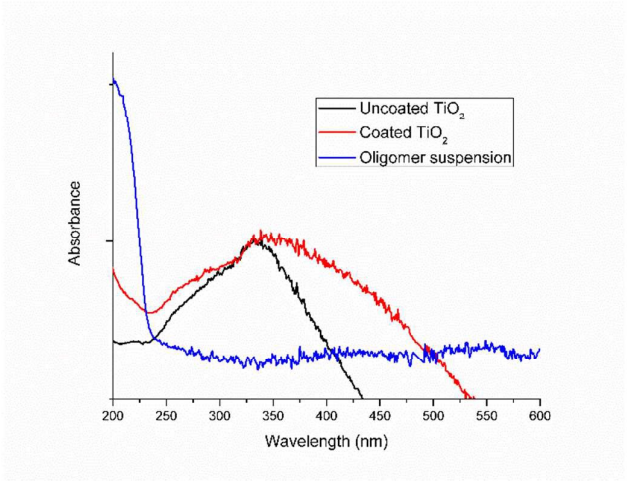

Figure 1. Optical absorption spectra of *oligomers* and uncoated and coated NP.

experiment. Figure 1 shows the absorption spectra of the coated and uncoated NP and the *oligomers*. As it was expected the uncoated NP and the *oligomers* adsorption bands were in the UV region. However,

in the coated NP spectrum, a wider absorption band was found extending up to the visible region.

The photoluminescence (PL) emission spectra were used to compare the recombination rate of photo-excited electron/hole pairs in the semiconductor materials. The results shown in Figure S5 exhibit similar excitonic PL emission bands for the coated and uncoated NP samples, indicating that the oligomers adsorbed on TiO2 NP did not generate any new emission peaks on the PL spectra.[17]

Besides, the PL emission intensity did not decrease upon NP coating with oligomers, meaning that the charge separation efficiency of the photo-excited e-/h+ pairs was not affected by the surface modifier and the e-/h+ recombination process was not altered. These results indicate that the enhancement in photocatalytic efficiency upon TiO2 coating would not be based on TiO2 bandgap energy narrowing.

Bringing together UV-visible and PL comparative behaviour of coated and uncoated TiO2, an alternative method of visible light activation of wide bandgap semiconductors must be considered for coated NP samples. This process, referred as the ligand-to-metal charge transfer (LMCT), is the sensitization by surface adsorbates that do not absorb visible light by themselves: the charge transfer induced by visible light occurs from the HOMO of adsorbates to the conduction band (CB) of TiO2. [16,30]

The oxidized adsorbate could be the radical cation of the N-heterocycle from the oligomers (stabilized by resonance), which could be regenerated by the recombination with the photoexcited electron (back electron transfer) or by reacting with suitable electron donors available in the medium.[16] Hydroxyl groups from the oligomer chain could also induce visible light photocatalytic activities. The HOMO level of the adsorbate relative to the CB edge is then a crucial factor in determining the visible light absorption in such LMCT complexes.

Effect of pH. The % decoloration of MO solution by the coated and uncoated NP as a function of media pH is shown in Figure 2. As it can be observed, the % decoloration decreased as the pH raised in both materials. The differences between coated and uncoated NP were

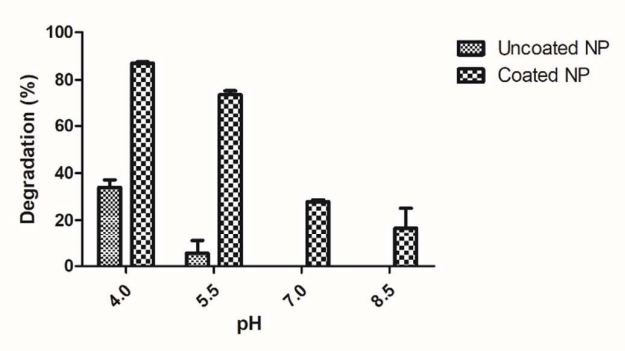

Figure 2. MO decoloration as a function of media pH

significant at every tested pH (p<0.05). The pH influence in the photocatalytic degradation process has multiple roles. First of all, the pH influences the ionization state of the catalyst surface. The point of zero charge of the uncoated TiO_2 is at pH 6.78 and is 6.30 for the coated TiO_2 (Figure S5). Thus, at lower values of pH, the TiO_2 surface presents a positive charge density and at higher values it is negatively charged. Since one of the most important steps in the photocatalysis process is the dye attraction to the catalyst surface, the analysis of this effect is relevant. At low pH the MO, negatively charged in the assayed pH range, is attracted to the surface by the positive charges, hence, the photocatalytic degradation process is more effective. At a pH higher than 6.8, as dye molecules are also negatively charged in alkaline media, their interaction is also expected to be affected by an increase in the density of TiO^- groups on the semiconductor surface. Previous studies also showed that the degradation rate of some azo dyes, such as MO, increased in an acidic media.[31–33] Moreover, both coated and uncoated NP were better photocatalysts in acid media provably because the free radicals released from h^+ on TiO_2 particles were more reactive at low pH values. At high pH values the hydroxyl radicals are rapidly scavenged which diminishes the probability to react with dyes.[34]

Effect of the initial dye concentration. Initial concentrations of MO were varied in the range of 0.0121–0.0595 mg L^{-1} and the results were exposed in Figure 3. As it could be observed, the % decoloration decreased with increasing initial concentration of the dye solution, specially at longer interaction times. This effect may be due to photon absorption by the dye in the more concentrated solutions before they reach the catalyst surface.[33]

When the initial concentration was low, and at short interaction times, the differences in % decoloration between coated and uncoated NP was evident. However, at 60 and 90 min of

View Article Online
DOI: 10.1039/C8NJ02332H

interaction, the difference in % decoloration between coated and uncoated NP was not significant (p>0.05). Meanwhile when the concentration was 0.0595 mg L^{-1}, the difference between them was significant (p<0.01), even at longer times.

Kinetics. The Langmuir-Hinshelwood (L–H) kinetics model is often used to describe the photocatalytic degradation of dyes (Eq.1).[11,35–37]

$$r = \frac{dC}{dt} = \frac{kKC}{1+KC} \qquad (1)$$

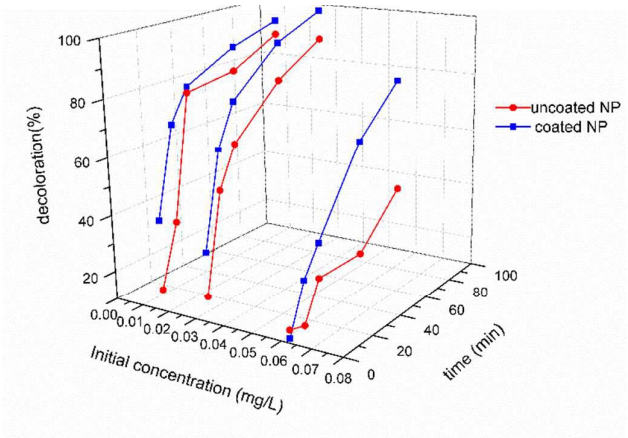

Figure 3. Decoloration of MO solutions photocatalyzed by coated or uncoated NP. Effect of initial dye concentration and time on % decoloration.

where r is the degradation rate of the reactant (mg L^{-1} min^{-1}), C the dye concentration (mg L^{-1}), t the illumination time, k the reaction rate constant (mg L^{-1} min^{-1}), and K is the adsorption coefficient of the reactant (L mg^{-1}).

If the initial dye concentration C_o is a millimolar solution the equation can be simplified to an apparent first-order equation (Eq 2):

$$\ln\frac{c_0}{C} = kKt = k_{app}\,t \qquad (2)$$

The graphic of ln C_o/C versus time represents a linear function which slope is the apparent first-order rate constant k_{app}.

Usually, first-order kinetics are appropriate for the description of studies performed at low concentrations of dyes and many studies were reasonably well fitted by this kinetic model [38–42].The L-H model was designed to explain the dependence of the reaction rate with the initial dye concentration. The L-H expressions are useful to describe the photocatalysis in any of the following four situations: (a) the reaction occurs when both the radicals and the dye are adsorbed to the surface, (b) the reaction takes place between a radical attached to the surface and the dye molecule is in the solution, (c) the reaction happen when the dye molecule is linked to the catalyst and the radical is in the solution and (d) the reaction occurs when

both species are in solution. In all the situations, the rate equation is similar to that derived from the L–H model, which has been useful to describe the process, although it is not possible to find out whether the process occurs on the surface in the solution or at the interface. [32]

The obtained parameters (Table 1) showed that the k_{app} and consequently, the reaction rate, are influenced by the initial concentration of the dye. In all cases k_{app} was higher for the coated NP than for the uncoated, which is indicative of an enhanced photocatalytic activity. This is also evidenced from the comparison of the k_{app} values progression against the initial concentration of the dye. In the case of the uncoated NP, this value diminished when the dye concentration raised, probably due to a decay in the penetration of light in the solution. When the coated NP were studied, the k_{app} for the two lowest concentration was similar and in the highest dye concentration, it diminished. Probably, due to the enhanced

Table 1. Langmuir–Hinshelwood model parameters

C_0 (mg.L^{-1})	Uncoated NPs k_{app} (s^{-1})	Coated NPs k_{app} (s^{-1})	k_{app} ratio (coated/un-coated)
(1.21 ± 0.02) x10^{-2}	(3.8 ± 0.5) x10^{-2}	(4.7 ± 0.4) x10^{-2}	1.25
(2.72 ± 0.03) x10^{-2}	(2.57 ± 0.09) x10^{-2}	(5.3 ± 0.2) x10^{-2}	2.05
(5.95 ± 0.01) x10^{-2}	(0.91 ± 0.05) x10^{-2}	(1.6 ± 0.1) x10^{-2}	1.78

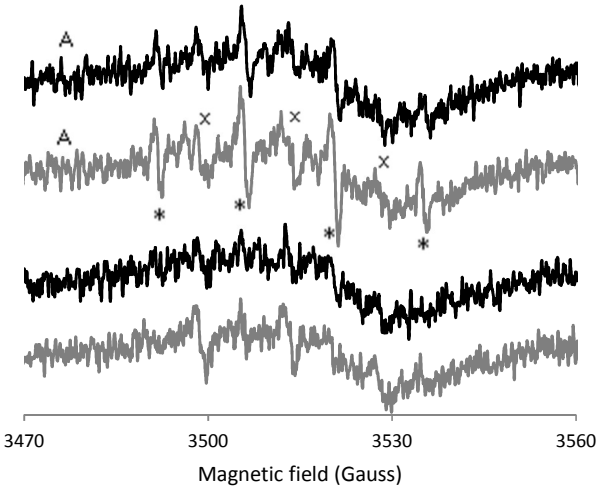

Figure 4. ESR spectra of supernatants of photocatalytic activation of NP systems in the presence of DMPO (A); identified adducts: quatriplet (*) and triplet (x). The spectra of the same systems in dark conditions (B). Black line: coated TiO_2 NP; grey line: uncoated TiO_2 NP.

photocatalytic activity of the coated NPs the effect of light penetration decrease at high MO concentration was attenuated by a higher rate of degradation. Figure 3 and Table 1 show that the photocatalytic efficiency of coated NP was particularly relevant at high MO concentrations, where the uncoated NP presented poor activity.

ESR experiments. Even if the catalytic mechanism described in Introduction section refers to adsorbed $OH^{\bullet}$, both the uncoated NP and the coated NP systems in water exposed to solar light released

View Article Online
DOI: 10.1039/C8NJ02332H

free radicals.[13] Most of these reactive species would stay attached to the catalyst surface, but some molecules would diffuse into the solution, being detected by spin trapping experiments with DMPO (Figure 4). For the supernatants of both coated and uncoated NP, similar spectra were observed. The simulation and fits of the experimental data allowed establishing the presence of DMPO/OH, a 1:2:2:1 quatriplet corresponding to the adduct formed by the hydroxyl radical ($OH^{\bullet}$) with the spin trap. The hyperfine coupling constants were: aN 14.5 G (spin: 1), and a_{H_β} 14.5 G (spin: ½). An interfering signal arisen from DMPO/OH degradation product was also detected as a triplet due to coupling with *N* nucleus.[43] In the absence of light, the signal of free radicals in the supernatants was practically negligible (Figure 4).

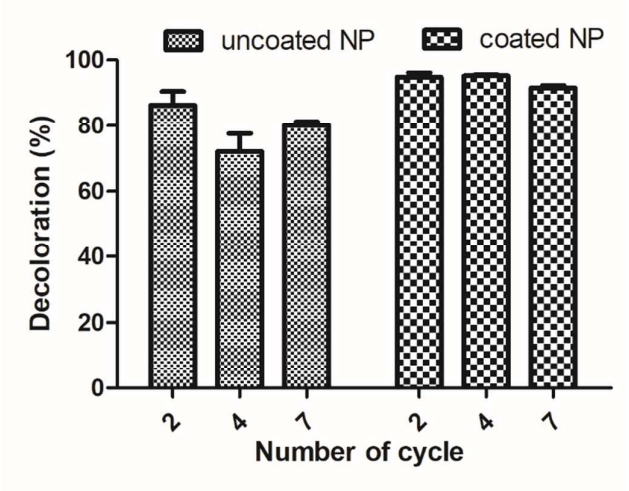

Figure 5. % Decoloration respect to the first cycle.

since the radical produced by both coated and uncoated NP was the same.

The ESR signal was more intense for uncoated NP photocatalytic system. These results indirectly suggest that the $OH^{\bullet}$ generated from h^{+} under light exposure would bind stronger to the photocatalytic surface coated with *oligomers* than to the uncoated TiO_2 particles. If the –IM residues were converted to radical cations by charge transference, the $OH^{\bullet}$ would form adducts with them.[19] Otherwise, the free radicals could stay adsorbed by weak interactions with the multiple hydrophilic functional groups of the *oligomers*. Taking into account that the MO molecules would be attracted by coated NP by means of IM^{+}/IMH^{+}, that $OH^{\bullet}$ would bind stronger on coated NP, and

that k_{app} was higher for coated NP systems, the higher efficiency of coated NP seems to be related to the proximity of both $OH^{\bullet}$ and MO in the heterogeneous photocatalytic system.

Intermediates and Toxicity. The completeness of the mineralization and the toxicity of the product was evaluated. According TOC results the mineralization was not complete, only a 18% of the MO was degraded with uncoated and coated NP. However, the toxicity assay established that the water treated with these NPs was not toxic. The percentage of seed growth was similar in distilled water (42%) and in the residual water from MO photocatalytic treatment with uncoated NP (50%) and coated NP (50%). These results showed that there was no generation of toxic compounds in any of the conditions tested.

Efficiency of the recycled catalyst. Photocatalysis is a clean technology, which normally does not involve any waste disposal problem. Furthermore, the catalysts generally can be recycled. In order to create an affordable material, it is essential that it can be used multiple operative cycles without sacrificing its efficiency and that the type of regeneration required does not imply an expensive process.

These materials were tested several times in order to evaluate if they undergo photocorrosion. As it is shown in Figure 5, the values of % decoloration between the cycle number were not significantly different (p>0.05). These results led us to conclude that the photocorrosion was negligible.

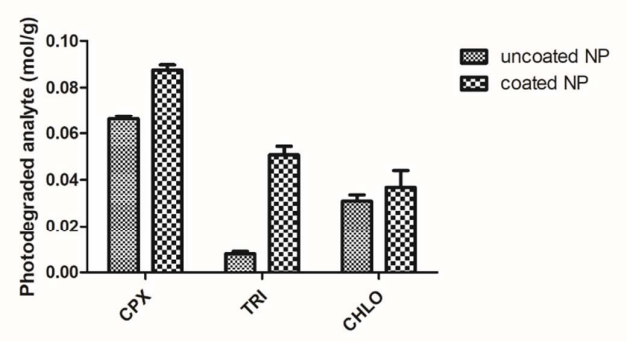

Figure 6. Photodegraded analyte after sunlight exposure. (CPX: ciprofloxacin, TRI: Trimethoprim and CHLO: Chloramphenicol).

Consequently, the use of these reusable coated NP may be considered as a cost-effective wastewater treatment since reuse diminishes the material costs and the photocatalytic source is solar-light. Besides, regeneration process implies a simple washing step and the agglomeration observed in coated NP promotes the sedimentation and easier removal from the aqueous media.

Versatility of the photocatalyst. The photocatalysis of the emergent contaminants ciprofloxacin, tocopherol and chloramphenicol was studied (Figure 6). In all the cases the photocatalysis of the pollutants was efficient. The differences between treated and untreated samples were significant for ciprofloxacin and tocopherol. Nevertheless, the concentration decreased in all the cases, showing that this material is useful for water treatment. Adsorption experiments in dark conditions showed that no adsorption occurred during 1 h of contact.

Photoluminescence (PL). Since the line shapes in the PL spectra from the samples are very similar (FigureS6), it can be concluded that the electronic state distributions of uncoated and coated NPs are similar within the band gap.

Conclusions

In this study an oligomer-based coating for TiO_2 nanoparticles was developed. This coating demonstrated to enhance the photocatalytic activity under solar light of the NP TiO_2 due to an enlargement of the absorption band into the visible range.

DOI: 10.1039/C8NJ02332H

The evidence indicates that the mechanism involved in the activation enhancement of the wide-bandgap semiconductor by solar light is the ligand-to-metal charge transfer (LMCT), a sensitization by surface adsorbates that do not absorb visible light by themselves.

The charge transfer induced by visible light would occur from the HOMO of oligomers to the conduction band (CB) of TiO2. In addition, the $OH^{\bullet}$ generated from h^{+} would bind stronger to the photocatalytic surface coated with *oligomers* than to the uncoated TiO_2 particles. The proximity of both $OH^{\bullet}$ and the dye MO on the particle surface would contribute to the higher efficiency in decolorization process.

The possibility of reusing this material makes the herein presented a cost-effective system for wastewater treatment. This material was tested against three emergent contaminants proving its efficacy. The main goal of this study is the generation of a new systems for water remediation of this type of pollutants without generating additional waste as in adsorption systems.

Conflicts of interest

There are no conflicts to declare.

Acknowledgements

M.E.V. is grateful for her posdoctoral fellowship granted by Consejo Nacional de Investigaciones Científicas y Técnicas. The authors are grateful with Instituto Nacional de Tecnología Industrial - Mecánica (INTI) for their assistance in SEM observations. This work was supported with grants from Universidad de Buenos Aires (UBACYT 20020130100780BA and 13-16/021), Consejo Nacional de Investigaciones Científicas y Técnicas (PIP 10-12/PIP 076) and Agencia Nacional de Promoción Científica y Tecnológica (PICT 2012 0716, PICT-2015-0714 and PICT 2016 1997).

Notes and references

1 V. Matamoros, Y. Rodríguez and J. Albaigés, *Water Res.*, 2016, **88**, 777–785.
2 B. Petrie, R. Barden and B. Kasprzyk-Hordern, *Occur. Fate Remov. Assess. Emerg. Contam. Water Water Cycle Wastewater Drink. Water*, 2015, **72**, 3–27.
3 X. Van Doorslaer, J. Dewulf, H. Van Langenhove and K. Demeestere, *Sci. Total Environ.*, 2014, **500**, 250–269.
4 A. Pal, K. Y.-H. Gin, A. Y.-C. Lin and M. Reinhard, *Sci. Total Environ.*, 2010, **408**, 6062–6069.
5 C. Hariharan, *Appl. Catal. Gen.*, 2006, **304**, 55–61.
6 R. Velmurugan and M. Swaminathan, *Sol. Energy Mater. Sol. Cells*, 2011, **95**, 942–950.
7 X. Xiang, L. Xie, Z. Li and F. Li, *Chem. Eng. J.*, 2013, **221**, 222–229.
8 B. Subash, B. Krishnakumar, M. Swaminathan and M. Shanthi, *Langmuir*, 2013, **29**, 939–949.
9 M. Šćepanović, M. Grujić-Brojčin, B. Abramović and A. Golubović, IOP Publishing, 2017, vol. 794, p. 012003.
10 H. Wang, H. Lin, Y. Long, B. Ni, T. He, S. Zhang, H. Zhu and X. Wang, *Nanoscale*, 2017, **9**, 2074–2081.
11 T. Sauer, G. C. Neto, H. Jose and R. Moreira, *J. Photochem. Photobiol. Chem.*, 2002, **149**, 147–154.
12 H. Dong, G. Zeng, L. Tang, C. Fan, C. Zhang, X. He and Y. He, *Water Res.*, 2015, **79**, 128–146.
13 G. Yang, Z. Jiang, H. Shi, T. Xiao and Z. Yan, *J. Mater. Chem.*, 2010, **20**, 5301–5309.
14 M. Wrona, W. Korytowski, M. Różanowska, T. Sarna and T. G. Truscott, *Free Radic. Biol. Med.*, 2003, **35**, 1319–1329.
15 S. G. Kumar and L. G. Devi, *J. Phys. Chem. A*, 2011, **115**, 13211–13241.
16 G. Zhang, G. Kim and W. Choi, *Energy Environ. Sci.*, 2014, **7**, 954–966.
17 Y.-C. Hsiao, C.-H. Su, C.-C. Hu and M. Rajkumar, *J. Electrochem. Soc.*, 2015, **162**, H93–H101.
18 F. Sannino, P. Pernice, C. Imparato, A. Aronne, G. D'Errico, L. Minieri, M. Perfetti and D. Pirozzi, *RSC Adv.*, 2015, **5**, 93831–93839.
19 I. Dogan, *Spectrosc. Lett.*, 1992, **25**, 1–11.
20 L. V. Lombardo Lupano, J. M. Lázaro-Martínez, N. M. Vizioli, D. I. Torres and V. Campo Dall'Orto, *Macromol. Mater. Eng.*, 2016, **301**, 167–181.
21 S. P. Pitre, T. P. Yoon and J. C. Scaiano, *Chem. Commun.*, 2017, **53**, 4335–4338.
22 D. J. Larsson, C. de Pedro and N. Paxeus, *J. Hazard. Mater.*, 2007, **148**, 751–755.
23 K. Dai, T. Peng, D. Ke and B. Wei, *Nanotechnology*, 2009, **20**, 125603.
24 M. Hamadanian, A. Reisi-Vanani and A. Majedi, *J. Iran. Chem. Soc.*, 2010, **7**, S52–S58.
25 J. M. Lázaro Martínez, M. F. Leal Denis, V. Campo Dall'Orto and G. Y. Buldain, *Eur. Polym. J.*, 2008, **44**, 392–407.
26 G. J. Copello, L. E. Diaz and V. Campo Dall' Orto, *J. Hazard. Mater.*, 2012, **217–218**, 374–381.
27 C. Shen, Y. Chang, L. Fang, M. Min and C. Xiong, *New J. Chem.*, 2016, **40**, 3588–3596.
28 W. Su, J. Zhang, Z. Feng, T. Chen, P. Ying and C. Li, *J. Phys. Chem. C*, 2008, **112**, 7710–7716.
29 Z. E. Allouni, M. R. Cimpan, P. J. Høl, T. Skodvin and N. R. Gjerdet, *Colloids Surf. B Biointerfaces*, 2009, **68**, 83–87.
30 V. Houlding and M. Gratzel, *J. Am. Chem. Soc.*, 1983, **105**, 5695–5696.
31 S. Sakthivel, B. Neppolian, M. Shankar, B. Arabindoo, M. Palanichamy and V. Murugesan, *Sol. Energy Mater. Sol. Cells*, 2003, **77**, 65–82.
32 I. K. Konstantinou and T. A. Albanis, *Appl. Catal. B Environ.*, 2004, **49**, 1–14.
33 M. A. Behnajady, N. Modirshahla and R. Hamzavi, *J. Hazard. Mater.*, 2006, **133**, 226–232.
34 J. Bandara, J. Mielczarski and J. Kiwi, *Langmuir*, 1999, **15**, 7680–7687.
35 J. Zhao and X. Yang, *Build. Environ.*, 2003, **38**, 645–654.
36 S. Chakrabarti and B. K. Dutta, *J. Hazard. Mater.*, 2004, **112**, 269–278.
37 N. Daneshvar, M. Rabbani, N. Modirshahla and M. A. Behnajady, *J. Photochem. Photobiol. Chem.*, 2004, **168**, 39–45.
38 Z. Khuzwayo and E. Chirwa, *J. Hazard. Mater.*, 2015, **300**, 459–466.
39 A. Shakouri, S. Z. Heris, S. G. Etemad and S. M. Mousavi, *J. Mol. Liq.*, 2016, **216**, 275–283.

View Article Online
DOI: 10.1039/C8NJ02332H

40 U. Habiba, M. S. Islam, T. A. Siddique, A. M. Afifi and B. C. Ang, *Carbohydr. Polym.*, 2016, **149**, 317–331.
41 S. Mosleh, M. Rahimi, M. Ghaedi, K. Dashtian and S. Hajati, *RSC Adv.*, 2016, **6**, 17204–17214.
42 S. Escobedo, B. Serrano, A. Calzada, J. Moreira and H. de Lasa, *Fuel*, 2016, **181**, 438–449.
43 J. Fontmorin, R. B. Castillo, W. Tang and M. Sillanpää, *Water Res.*, 2016, **99**, 24–32.

View Article Online
DOI: 10.1039/C8NJ02332H

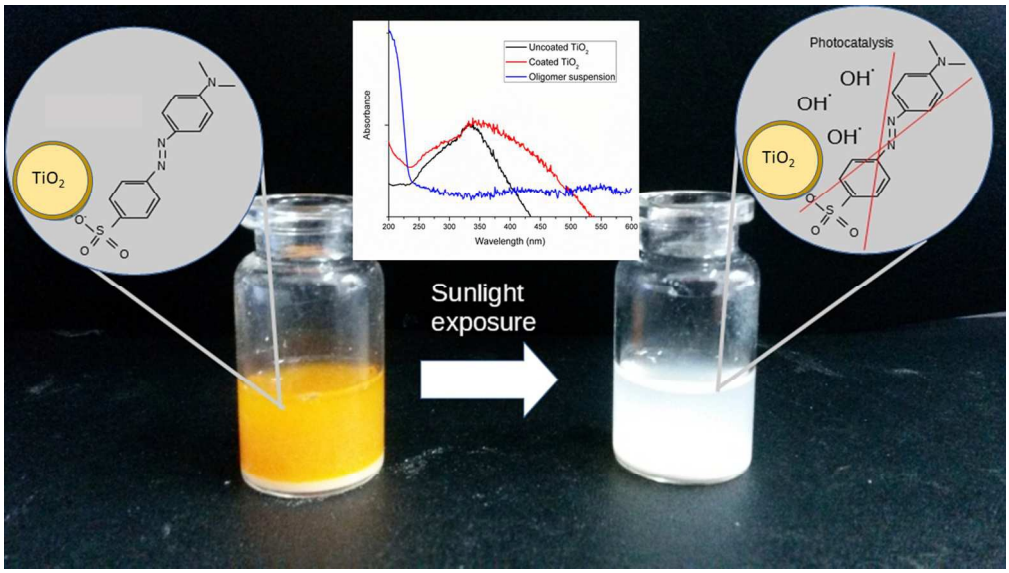

338x190mm (96 x 96 DPI)